Black-out diesel engine operation modelling for the CHPP start-up

Dušan Strušnik
Energetika Ljubljana d.o.o.,
TE-TOL Unit, Toplarniška ulica 19
SI-1000 Ljubljana, Slovenia
dusan.strusnik@gmail.com
https://orcid.org/0000-0003-2531-3081

Marko Agrež
Energetika Ljubljana d.o.o.,
TE-TOL Unit, Toplarniška ulica 19
SI-1000 Ljubljana, Slovenia
marko.agrez@energetika.si

Jurij Avsec
University of Maribor
Faculty of Energy Technology
Hočevarjev trg 1
SI-8270 Krško, Slovenia
urij.avsec@um.si

Abstract

Modelling power plants using real process data is crucial in determining the cost-effectiveness and flexibility of systems. The quality of the elaborated model is determined with the validation of the model, which can also give results for the operating regimes of the plant, which are not often used in practice. In this way, also the operation and responsiveness of power plants outside the range of planned operation are determined. The model simulates the operation of a diesel engine (DE) required to start a combined heat & power plant (CHPP) from a black-out or loss of the electrical power network supply. The model is made on the basis of data provided by the manufacturer and the measured DE data. The results of the model enable detailed insight into the characteristics of the DE behaviour at different operating regimes. The economic and ecological rationale ranges of operation of the DE can be determined from the characteristics of operation. The results of the model show that the DE operates with a 41.72% average efficiency, consumes from 0.114 kg/s of diesel fuel for its operation and up to 3.68 kg/s of air, the air ratio ranges from 2.2 to 2.5. DE develops shaft power up to 2170 kW.

Keywords: Air-Fuel Equivalence Ratio, Black-Out, Diesel Engine, Thermal Efficiency, Shaft Power

I. INTRODUCTION

Optimization of thermal power systems and ecological awareness is a key development strategy of larger thermal power facilities. Despite the fact that the production of electricity with low-carbon or non-carbon technology is on the rise, it will not be possible to completely avoid the production of electricity by burning fossil fuels. One of the most efficient methods to convert fossil resources or chemically bound energy of gaseous and liquid fuels into electricity is the use of gas turbines.

IEECP'22, July 21-22, 2022, Oxford, United Kingdom

The production of electricity using a gas turbine and an electric generator can be ensured in the open cycle [1], where hot flue gases after expansion are released through the chimney directly into the atmosphere. The disadvantage of this process is the relatively low efficiency of the plant, which in practice ranges from 30% to 40%. If we want to improve the efficiency, the open cycle is upgraded with a boiler, heat recovery steam generator [2] and a steam turbine that takes the generated steam from the said boiler and drives its electric generator. The really useful efficiencies achieved in this process range from 50% to 60%. Such a process is called a combined cycle gas turbine [3]. If we have the option of heat extraction, the total energy efficiency of the plant can exceed 85%. The operation of such an energy system is also called combined heat & power [4].

In addition to achieving high energy efficiency, the combined cycle gas turbine process is also characterized by its universality. Simultaneously with the production of heat and electricity, both generators powered by gas and steam turbines can be included in the system of balancing the production and consumption of electricity. The said balancing is performed by the operators who operate the transmission high-voltage system. The entire Slovenian electricity system is included in the European interconnection system or the European Network of Transmission System Operators for Electricity [5]. Individual networks, connected to the interconnection by means of the interaction of synchronous generators and system regulations of electric frequency, ensure the quality of operation of power systems. This means that the power hubs, where the dividing line between the transmission and distribution of electricity begins, are constantly supplied. In practice, however, this balancing means that electricity must be produced practically at the same time as the random consumer connects to the power supply.

The combined cycle gas turbine installation is very efficient in providing regulation or ancillary services for the needs of working or operation of the electricity transmission system. Its fast response and gradient of increasing the electric power of the generator connected to the gas turbine, allows a very fast adjustment of electricity production to its consumption. The system is designed in such a way that it also enables the quick start of cold units. The advantage of fast start-up of a combined cycle gas turbine is especially pronounced when starting from a voltage-free state of the power system, since the combined cycle gas turbine is able to ensure electricity production in a very short time and thus to maintain the frequency of the power grid in a smaller island, which expands by adding the resources.

In the event of a power system breakdown resulting in a black-out, the combined cycle gas turbine needs an energy source to start the auxiliary devices needed to start the system. Most often, these auxiliary devices are internal combustion engines that drive a starting electric generator. In practice, DEs have proven to be reliable resources. The task of the DE is therefore to provide, in the case of black-out, the electricity needed to start the combined cycle gas turbine.

The paper is designed in such a way that the characteristic data and components of the DE are presented first. Then the presentation of the simulation model of the DE operation follows, followed by the presentation of the results of the simulation model. Finally, a summary with the most important findings is presented.

II. DA CHARACTERISTICS AND COMPONENTS

The DE for CHPP start-up at black-out is turbocharged, aftercooled and four-stroke engine and operates with a constant revolution frequency of 1500 min-1, which is required to drive the generator. The basic characteristic data of the DE are shown in Table 1.

Table 1. The basic characteristic data of DE, industrial engine with constant speed [5]

Manufacturer	Mitsubishi
Model	S16R2-PTAW
Engine type	four-stroke, diesel
Cylinder configuration	16 / 60 °V
Maximum output power	2167 kW
Engine speed	1500 min^{-1}
Aspiration and cooling	Turbocharged and aftercooled
Total displacement	79.90 litters
Bore and stroke	170 mm x 220 mm
Compression ratio	14:1
Fuel consumption at full load	0.114 kg/s
Cooling system	Water-cooled
Combustion system	Direct injection
Fuel injection system	Pump – line - nozzle

Figures 1 and 2 were taken during the first phase of the DE tests. Figure 1 shows the right side of the body of 60° V16 DE. Each side of DE therefore has 8 cylinders.

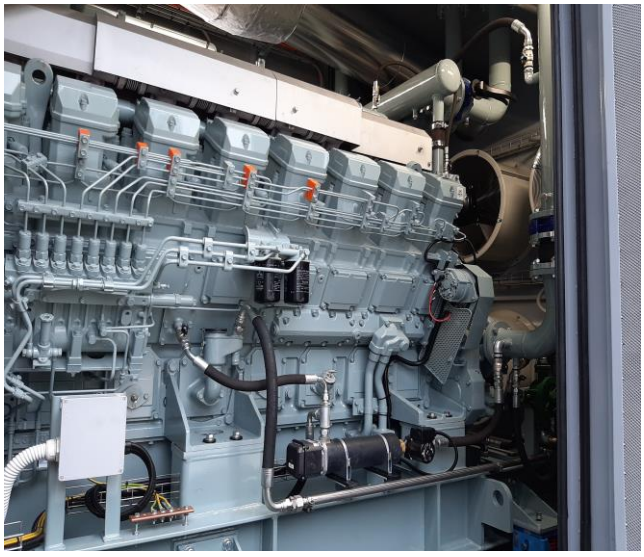

Figure 1. The right side of the body of 60° V16 DE.

Figure 2 shows the first trial run. The left DE is operating and the right DE is in the phase of the first start-up trial run.

Figure 2. DE first start-up trial run.

Figure 3 shows the DE view from the left side with the basic components marked. Table 2 presents the basic components of DE from Figure 2.

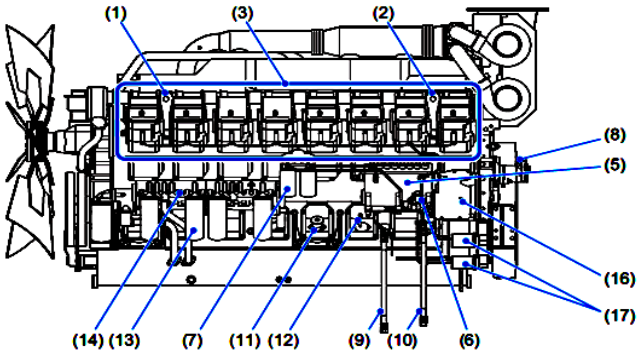

Figure 3. View of the DE from the left side with components [7].

Table 2. The basic characteristic data of the DE, industrial engine with constant speed [7]

	No.	Name		No.	Name
Engine body	(1)	Front hanger	Lubrication system	(11)	Oil filler
	(2)	Rear hanger		(12)	Oil level gauge
	(3)	Cylinder head		(13)	Oil filter
	(4)	Manual turning gear		(14)	Oil cooler
Fuel system	(5)	Fuel injection pump	Cooling system	(15)	Coolant inlet
	(6)	Priming pump		(16)	Coolant drain cock
	(7)	Fuel filter	Starting system	(17)	Starter
	(8)	Fuel control link	Electrical system	(18)	Alternator
	(9)	Fuel inlet			
	(11)	Fuel return port			

The left side of Figure 4 shows the view of the DE from the front with the basic components marked. The right of Figure 4 shows the view of the DE from the back, where the basic components are also marked, and Table 3 presents the basic components of the DE from Figure 3.

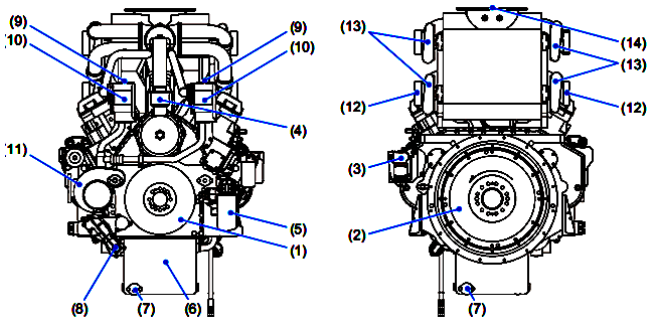

Figure 4. DE front view and DE rear view [7].

Table 3. The basic characteristic data of the DE, industrial engine with constant speed [7]

	No.	Name		No.	Name
Engine body	(1)	Damper	Cooling system	(9)	Coolant outlet
	(2)	Flywheel		(10)	Thermostat case
Fuel system	(3)	Governor actuator		(11)	Water pump
Lubrication system	(4)	Breather	Inlet and exhaust systems	(12)	Intake port
	(5)	Bypass oil filter		(13)	Turbocharger
	(6)	Oil pan		(14)	Exhaust outlet
	(7)	Engine oil drain port			
	(8)	Oil pump			

The remaining necessary DE data required for the production of a quality model are shown in Table 4.

Table 4. The remaining DE data, industrial engine with constant speed [7]

ENGINE	
Number of cylinders	16
Bore	170 mm
Stroke	220 mm
Displacement	79.9 litres
Brake power without fan	2209 kW
Brake mean effective pressure	21.1 bar
Mean piston speed	11 m/s
Maximum regenerative power	152 kW
PERFORMANCE DATA	
Steady state speed stability band at any constant load - electric governor	± 0.25 %
Maximum overspeed capacity	1750 rpm
Moment of inertia of rotating components	33.22 kg*m^2
Cyclic speed variation with flywheel at 1500 rpm	1/182
AIR INLET SYSTEM	
Maximum Intake Air Restriction	0.064 bar
EXHAUST SYSTEM	
Maximum Allowable Back Pressure	0.059 bar
LUBRICATION SYSTEM	
Oil Pressure	5 bar
Maximum oil temperature	105 °C
Oil capacity of standard pan	240 litres
COOLING SYSTEM	
Coolant capacity of jacket	157 litres
Coolant capacity of air cooler	33 litres
Maximum external friction head at engine outlet	0.34 bar
Standard thermostat (modulating) range of jacket	71 °C ~ 85 °C
Standard thermostat (modulating) range of air cooler	42 °C ~ 55 °C
Maximum coolant temperature at engine inlet	75 °C
Maximum coolant temperature at engine outlet	83 °C
Minimum coolant expansion space	10 %
Maximum coolant temperature at air cooler inlet	45 °C
FUEL SYSTEM	
Fuel Injector	Mitsubishi PS8 Type × 2
Maximum suction head of feed pump	0.1 bar
Maximum static head of return & leak pipe	0.2 bar
STARTING SYSTEM	
Battery charging alternator	24 V, 35 Ah
Starting motor capacity	24 V, 7.5x2 kW

III. DE OPERATE SIMULATION MODEL

The DE operate simulation model consists of three units: the DE input data unit, the DE calculation unit and the results report unit. A schematic representation of the architecture of the simulation model is shown in Figure 5.

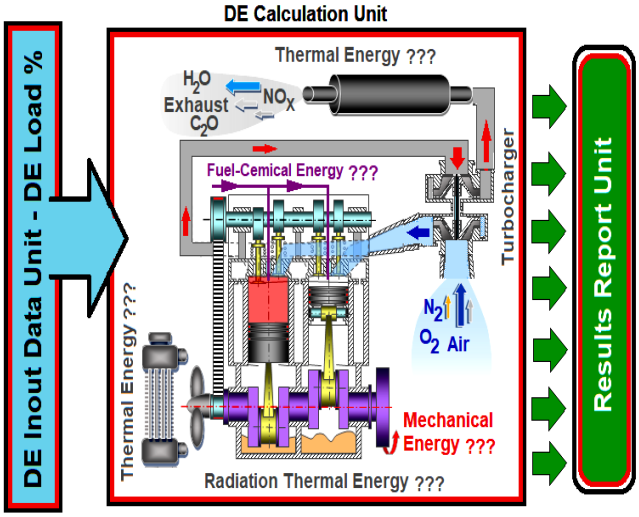

Figure 5. Schematic representation of the simulation model.

Using input data of the DE loads, the DE calculation unit calculates: the diesel fuel consumption, the combustion air volume, the air ratio, the exhaust gas quantity, the cooling water quantity, etc. In addition to the stated values, the DE calculation unit also calculates the following values: the mechanical power of the engine shaft, the thermal power of exhaust gases, the thermal power of cooling water, the radiated heat released into the environment and the thermal power of the oil cooler. The DE calculation unit calculates the stated values using the thermodynamic equations and equations that were generated with the help of realistically

measured data of the working of DE in dependence on load. The mass flow of diesel fuel in dependence on the load is calculated by the DE calculation unit using equation [8]:

$$\dot{m}_{fuel} = \frac{m \cdot N_{cysm} \cdot n_e}{60 \cdot N_{nst}} \quad (1)$$

where $\dot{m}_{fuel}$ is the mass flow of diesel fuel for the working of DE, m is the cycle fuel injection quantity, N_{cysm} is the number of cylinders, n_e is the engine speed, N_{nst} and is the number of engine strokes. The mass flow of exhaust gases in dependence on the load is calculated by the DE calculation unit using a polynomial equation of the second degree, which was generated using the measured data:

$$\dot{m}_{ex} = \frac{(0.01522 \cdot DE_{load}{}^2 + 2.545 \cdot DE_{load} + 91.72) \cdot 0.457}{60} \quad (2)$$

where $\dot{m}_{ex}$ is the mass flow of exhaust gases from the DE and DE_{load} is the load of the DE. The mass flow of air required for the working of the DE is the difference between the mass flow of exhaust gases and the mass flow of diesel fuel and is calculated by the DE calculation unit using equation [9]:

$$\dot{m}_{air} = \dot{m}_{ex} - \dot{m}_{fuel} \quad (3)$$

where $\dot{m}_{air}$ is the mass flow of air for the working of the DE. However, now that the actual mass flows of air and fuels required for the working of the DE are known, the calculation unit can calculate the air-fuel equivalence ratio (ʎ) [10]:

$$\lambda = \frac{AFR_{actual}}{AFR_{stoich}} = \frac{AFR_{actual}}{14.7} \quad (4)$$

where ʎ is the air-fuel equivalence ratio, AFR_{actual} is the air-fuel ratio at actual conditions and AFR_{stoich} is the air-fuel ratio at stoichiometry conditions. The power of the shaft developed by the DE is calculated by the calculation unit using the measured value of the electric power of the generator and using the efficiency of the generator [11]:

$$P_{shaft} = P_{gen} \cdot \eta_{gen} \quad (5)$$

where P_{shaft} is the power of the shaft of DE and η_{gen} is the efficiency of the generator of DE. The thermal power of the exhaust gases is calculated by the DE calculation unit using equation [12]:

$$P_{ex} = \dot{m}_{ex} \cdot c_{p-ex} \cdot T_{ex} \quad (6)$$

where P_{ex} is the thermal power of the exhaust gases from the DE, c_{p-ex} is the specific heat of the exhaust gases and T_{ex} is the exhaust gas temperature obtained from the measurements made. In a similar way, with the help of the measured data, the calculation unit also calculates the thermal power discharged from the DE by means of cooling water and oil cooler [13]:

$$P_{cool} = \dot{m}_{cool} \cdot c_{p-cool} \cdot (T_{cool-out} - T_{cool-in}) \quad (7)$$

$$P_{oil} = \dot{m}_{oil} \cdot c_{p-oil} \cdot (T_{oil-out} - T_{oil-in}) \quad (8)$$

where P_{cool} is the thermal power of cooling water discharged from the DE, $\dot{m}_{cool}$ is measured mass flow of cooling water trough the DE, c_{p-cool} is the specific heat of the cooling water, $T_{cool-out}$ is the measured temperature of cooling water from the DE, $T_{cool-in}$ is the measured temperature of cooling water into the DE, P_{oil} is the thermal power of oil cooler discharged from the DE, $\dot{m}_{oil}$ is the mass flow of oil trough the DE, $T_{oil-out}$ is the temperature of oil from the DE and T_{oil-in} is the temperature of oil into DE. The heat released from the DE into the environment in the form of radiation is calculated by the calculation unit using the polynomial equation of the second degree generated by the data provided by the manufacturer of DE [6]:

$$P_{rad} = 0.002888 \cdot DE_{load}{}^2 + 1.192 \cdot DE_{load} + 17.03 \quad (9)$$

where P_{rad} is the radiative heat of the DE. The efficiency of the DE is calculated by the calculation unit using the equation [14]:

$$\eta = \frac{\sum P_{use}}{P_{fuel}} \cdot 100\% = \frac{\sum P_{use}}{\dot{m}_{fuel} \cdot se_{fuel} \cdot 3600} \cdot 100\% \quad (10)$$

where η is the efficiency of the DE, $\sum P_{use}$ is the sum of all the usefully consumed power of the DE, P_{fuel} is the power supplied by the fuel and se_{fuel} is the specific energy of diesel fuel.

IV. SIMULATION MODEL RESULTS

The results of the model are shown at a constant revolution frequency of the DE, which is 1500 min^{-1}, since the DE is used to drive a generator that always operates at a constant rpm. The results of the model are designed so that the flow characteristics of air, fuel, exhaust gases and the distribution of the generated power of the DE in depending on the DE load are presented first. This is followed by a display of the generated power of the DE shaft, the diesel fuel combustion temperature and the air-fuel ratio (AFR) in dependence on the DE load. Then, the air and exhaust gas temperatures are shown, and finally the generator useful efficiencies and the DE useful efficiencies in dependence on the DE load are shown.

From Figure 6 (a), it is evident that the mass flow of the diesel fuel for driving the DE ranges from 0.035 kg/s at 30% load of the DE and up to 0.114 kg/s at 100% load of the DE. The mass flow of air entering DE ranges from 1.35 kg/s at 30% DE load up to 3.68 kg/s at 100% DE load. The mass flow of exhaust gases is the sum of the mass flow of fuel and the mass flow of air entering DE. The air-fuel equivalence ratio or ʎ decreases with increasing of the DE load and ranges from 2.2 to 2.5. This means that DE works from 120% to 150% of excess air, which has a positive ecological impact as it reduces the sootiness of exhaust gases.

Figure 6 (b) shows the power supplied by diesel fuel and the distribution of generating power of the DE in dependence on the load. The supplied power of diesel fuel amounts from

1550 kW to 4880 kW and increases in dependence on the DE load. Also, as the DE load increases, the power of the engine shaft increases and ranges from 480 kW to 2170 kW. The power of exhaust gases of the DE ranges from 730 kW to 1820 kW. The cooling water power of the DE ranges from 250 kW to 640 kW. Radiation through the DE housing ranges from 55 kW to 165 kW depending on the DE load. The heat dissipated from the oil cooler to the surroundings also increases with increasing the DE load and ranges from 30 kW up to 84 kW.

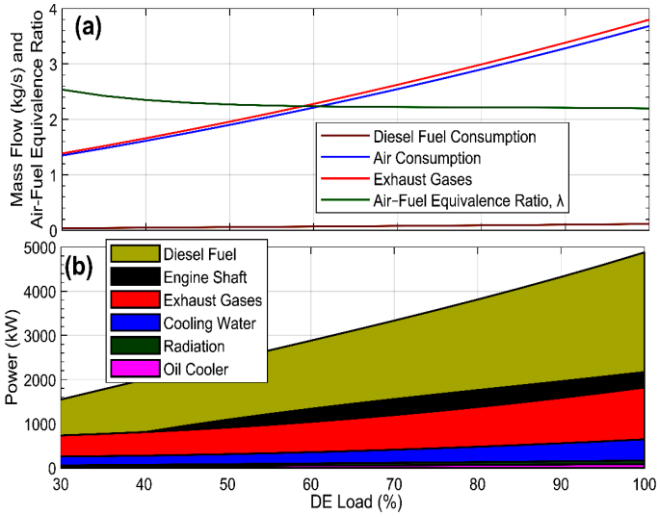

Figure 6. (a) the flow characteristics of air, fuel, exhaust gases and air-fuel equivalence ratio or ƛ of the DE; (b) the power supplied by the diesel fuel and the distribution of the power generated by the DE.

Figure 7 (a) shows the power of the DE shaft and the combustion temperatures in dependence on the DE load. At 30% of the DE load, the generated power of the DE shaft is 475 kW and as the DE load increases, the generated power of the DE shaft also increases. At 100% of the DE load, the power of the DE shaft amounts to 2164 kW. The combustion temperature increases up to 60% of the DE load, where it amounts to 1755 °C, and with increasing the DE load, it starts to decrease and at 100% of the DE load it is 1521 °C. At 30% of the DE load, the combustion temperature is 1650 °C.

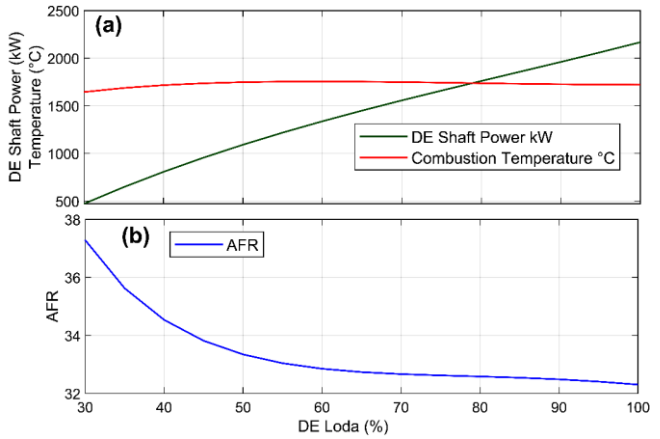

Figure 7. (a) power of the DE shaft and combustion temperature in dependence on the DE load; (b) AFR in dependence on the DE load.

However, from the diagram in Figure 7 (b) it is evident that the AFR depends on the DE load. At 30% of the DE load, the AFR value is at its maximum of 37 and decreases with increasing the DE load. At 100% of the DE load, the ARF decreases to the value of 32. The ratios of AFR and ƛ indicate that the DE is working with a high excess of air. The working of the DE with excess air has positive effects on the environment in terms of minimizing the generation of soot particles in exhaust gases or reducing sootiness.

The DE therefore work in the range with a high air excess, and the DE power is regulated by the amount of injected fuel. When increasing the DE load, the more fuel is injected and vice versa. As fuel injection increases, however, the mixture of air and fuel becomes richer, making it increasingly difficult to mix fuel and air in the combustion chamber. Due to the increasing difficulty of mixing fuel and air, the efficiency of combustion begins to decrease, but not the power of the DE. There is an upper limit at which the reduction in combustion efficiency can no longer be compensated by the addition of fuel. In this way, the optimal AFR which is in the range between poor and rich mixture is determined. The efficiency of the combustion in DE in dependence on ƛ is shown in Figure 8.

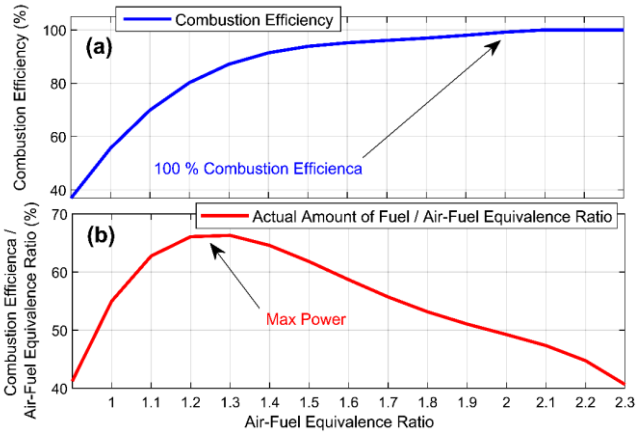

Figure 8. (a) The efficiency of the combustion in DE in dependence on the air-fuel equivalence ratio, or ƛ; (b) the ratio of ″combustion efficiency / air-fuel equivalence ratio″ in dependence on the air-fuel equivalence ratio, or ƛ.

It is evident from Figure 8 (a) that the efficiency of combustion in DE is achieved only at the air-fuel equivalence ratio, or ƛ = 2, which means that efficient combustion in DE is achieved when ƛ > 2. However, increasing ƛ decreases the power of the DE. DE develops maximum power ƛ = 1.25, which can be seen from the diagram in Figure 8 (b). The ratio of ″combustion efficiency / air-fuel equivalence ratio″ in Figure 8 (b) represents the actual amount of fuel consumed by the DE. Due to the generation of a huge amount of soot, the ƛ = 1.25 is used in DM only in a racial context. Serial production DE work for normal use ƛ > 1.65 [15].

The results of the model also give the results of the air-exhaust gases temperature profile in dependence on the DE load. It is evident from Figure 9 that the air temperature after the intercooler ranges from 70 °C to 98 °C. The maximum air

temperature after the intercooler is reached at 45% of the DE load, and then begins to decrease. At 100% of the DE load, the air temperature after the intercooler is the lowest and amounts to 70 °C. The lower air temperature after the intercooler has a positive effect on the work done by the DE, as the air density increases with decreasing temperature, which means that a larger mass of air can be brought to the same constant volume.

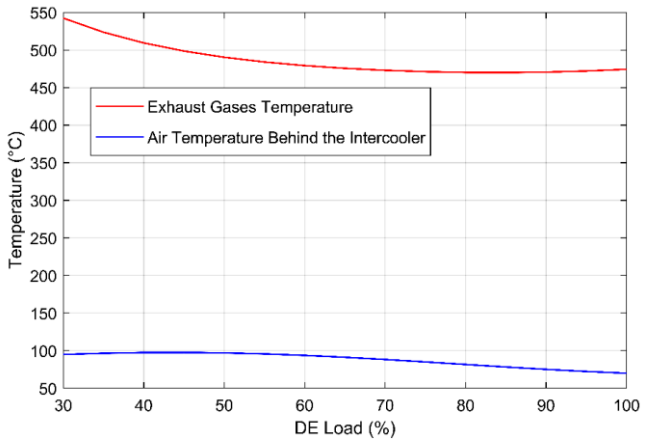

Figure 9. The air-exhaust gas temperature profile in dependence on the DE load.

The change in exhaust gas temperature in dependence on the DE load is also evident in Figure 9. Exhaust gas temperature ranges from 470 °C to 545 °C. The lowest exhaust gas temperature is reached at 80% of the DE load and the highest exhaust gas temperature is reached at the minimal DE loads.

Figure 10 shows the efficiency of the generator and the efficiency of the DE at different loads. From Figure 10 (a), it is evident the efficiency of the generator, which ranges from 94% of the minimal DE load to 96% at 70% of the DE load, then the generator efficiency starts to decrease and at 100% of the DE load it is 95.7%. The efficiency of DE ranges from 28% at minimal load to 45% at 60% of the load. Then the efficiency of DE starts to decrease and at 100% of load it is 42.5%.

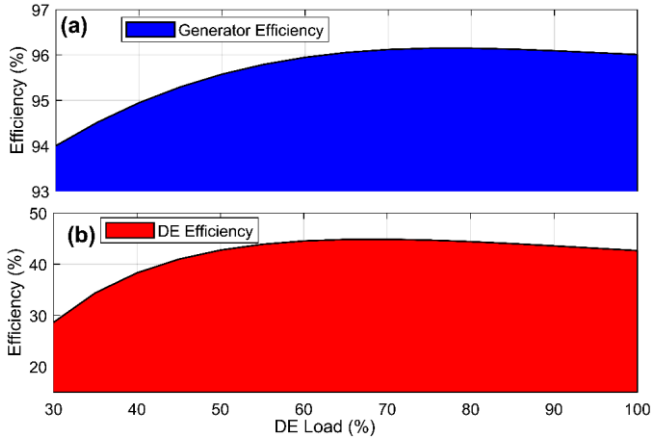

Figure 10. (a) generator efficiency in dependency of the DE load; (b) DE efficiency in dependency on load.

V. CONCLUSIONS

In this paper, the model and modelling results of the DE for the CHPP start-up at black-out are presented. The model consists of several sub-models, each sub-model has its own task. The most important sub-model is the calculation unit in which the mathematical equations are written, which are needed to accurately and precisely present the results. The quality of the model, however, depends on the quality of the set of measured data from the operating system, as this data is a key link that serves in generating mathematical expressions written in the calculation unit. The results of the model show that the DE works with a large excess of air λ = 2.2, which is mainly attributed to ecological aspects, namely the reduction of soot in exhaust gases Particular attention should also be paid to the efficiency of the DE, as the heat of the exhaust gases, as well as the heat of the cooling water, is discharged into the environment. Therefore, the efficiency varies depending on the DE load, ranging from 20% of the minimal DE load to 45% at 60% of the DE load. By using the heat of the exhaust gases and the heat of the cooling water of the DE, cogeneration operation for the production of heat and electricity, the efficiency of the DE can be greatly improved. In the case of the use of exhaust gas heat and cooling water, the DE could operate not only in the event of an electric eclipse, but also in cases of high electricity needs of the electricity system, since the price of electricity is high at that time.

VI. REFERENCES

[1] L. Chen, B. Yang, H. Feng, Y. Ge, S. Xia, "Performance optimization of an open simple-cycle gas turbine combined cooling, heating and power plant driven by basic oxygen furnace gas in China's steelmaking plants," Energy, 2020; 203, p. 117791. https://doi.org/10.1016/j.energy.2020.117791.

[2] M. A. Elhosseini M. A, A. Ahmed shams El-din, H. A. Hesham Arafat Ali, A. Abraham, "Heat recovery steam generator (HRSG) three-element drum level control utilizing Fractional order PID and fuzzy controllers," ISA Transactions, 2021. https://doi.org/10.1016/j.isatra.2021.04.035.

[3] A. Aya, A. Barakat, H. Jad, j. H. Diab, N. S. Badawi, W. S. B. Nader, C. J. Mansour, "Combined cycle gas turbine system optimization for extended range electric vehicles," Energy Conversion and Management, 2020; 226, p. 113538. https://doi.org/10.1016/j.enconman.2020.113538.

[4] G. Hou, L. Gong, B. Hu, T. Huang, H. Su, C. Huang, G. Zhou, S. Wang, "Flexibility oriented adaptive modeling of combined heat and power plant under various heat-power coupling conditions," Energy, 2021; p. 122529. https://doi.org/10.1016/j.energy.2021.122529.

[5] European Network of Transmission System Operators for Electricity, https://www.entsoe.eu/.

[6] Mitsubishi heavy industries, Mitsubishi diesel engine S16R2-PTAW, powerful and reliable, https://engine-genset.mhi.com.

[7] C. Maraffi, M. Turchiarelli, L. Sepe L, "Black start diesel generator. Operation & maintenance manual," Mitshubishi diesel engine S16R, 2018, No. 29001-00120.

[8] T. Ouyanga, Z. Su, B. Gao, M. Pan, N. Chen, H. Huang, "Design and modeling of marine diesel engine multistage waste heat recovery system integrated with flue-gas desulfurization," Energy Conversion and Management, 2019; 196, pp. 1353–1368. https://doi.org/10.1016/j.enconman.2019.06.065.

[9] D. Strušnik, "Integration of machine learning to increase steam turbine condenser vacuum and efficiency through gasket resealing and higher heat extraction into the atmosphere," International Journal of Energy Research, 2021. https://doi.org/10.1002/er.7375.

[10] I. Arsie, R. Di Leo, C. Pianese, M. De Cesare, "Estimation of in-cylinder mass and AFR by cylinder pressure measurement in automotive Diesel engines," Proceedings of the 19th World Congress, The International Federation of Automatic Control, 2014; pp. 24-29.

https://doi.org/10.3182/20140824-6-ZA-1003.01602.

[11] . J. D. Forero, "Energy, exergy and environmental assessment of partial fuel substitution with hydroxy powered by a thermoelectric generator in low displacement diesel engines," Cleaner Engineering and Technology, 2021; 3, p. 100086.
https://doi.org/10.1016/j.clet.2021.100086.

[12] H. Li, Y. Li, P. Zhao, J. Wang, G. Zhang, X. Qin, J. Chen, "Optimization research on the off-design characteristics of partial heating supercritical carbon dioxide power cycle in the landfill gas exhaust heat utilization system," Applied Thermal Engineering, 2021; 199, p. 117585.
https://doi.org/10.1016/j.applthermaleng.2021.117585.

[13] Y. Cao, W. W. L. Mihardjo, M. Dahari, A. M. Mohamed, H. Ghaebi, T. Parikhani, "Assessment of a novel system utilizing gases exhausted from a ship's engine for power, cooling, and desalinated water generation," Applied Thermal Engineering, 2021; 184, p. 116177.
https://doi.org/10.1016/j.applthermaleng.2020.116177.

[14] M. Oikawa, Y. Kojiya, R. Sato, K. Goma, Y. Takagi, Y. Mihara, "Effect of supercharging on improving thermal efficiency and modifying combustion characteristics in lean-burn direct-injection near-zero-emission hydrogen engines," International Journal of Hydrogen Energy, 2021.
https://doi.org/10.1016/j.ijhydene.2021.10.061.

[15] H. H. Schrekn, L. B. Berger, "Composition of Diesel Engine Exhaust Gas," American Journal of Pblic Health, 1941.